

Further, no differences in the mean or SD signal intensity in any of the muscle regions were noted at baseline (data not shown). Changes in ACSAs over 2 years also did not significantly differ between progressor and non-progressor knees (Table 1). When stratifying comparisons for cases with little baseline pain (WOMAC score of 0–1; $n=7$) vs. those with a score of 5–8 ($n=8$), the findings were similar (data not shown).

Conclusions: Progressor (case) and non-progressor (control) knees in this study were carefully selected from a large subsample, based on two independent measures of structural OA progression (MRI cartilage loss and JSW reduction in X-rays). Further, cases and controls were carefully matched for measures known to be associated with progression or with muscle area. The results of this exploratory study do not provide support that, once radiographic knee OA is established, baseline or longitudinal changes in thigh muscle ACSAs or strength predict (or are associated) with structural progression.

438 EVALUATION OF THE DEPENDENCY OF GLYCOSAMINOGLYCAN (GAG) CHEMICAL EXCHANGE SATURATION TRANSFER (GAGCEST) IMAGING ON CARTILAGE GAG CONTENT IN THE ANKLE AT 3 T

B. Schmitt, M. Brix, J. Hofstaetter, R. Windhager, S. Trattnig, S. Domayer. *Med. Univ. of Vienna, Vienna, Austria*

Purpose: This study was performed to evaluate the feasibility of gagCEST imaging in the ankle on a clinical 3-Tesla MR scanner. The dependency of gagCEST signal on cartilage GAG content was investigated by comparison of MRI data with quantitative biochemical assessment of cartilage GAG content.

Methods: The study comprised 7 ankle samples from human cadavers, which were examined on a clinical 3 T MR System with a standard knee coil. PD_w were acquired with turbo spin-echo (TSE) imaging and fatsat (FS) in the sagittal plane ($T_E=26$ ms, $T_R=4000$ ms, resolution= $0.4 \times 0.4 \times 3$ mm³). GagCEST imaging was performed using a segmented 3D RF-spoiled gradient-echo (GRE) sequence ($T_E=3.49$ ms, $T_R=9.1$ ms, resolution= $0.6 \times 0.6 \times 3.3$ mm³, scan time 10:30 min). Selective RF presaturation was achieved using a series of 3 Gaussian RF-pulses with pulse duration $\tau_p=100$ ms, an interpulse delay $\tau_d=10$ ms and a B_1 of 2.6 μ T. Z-spectra from images were corrected for B_0 inhomogeneities on a pixel-by-pixel basis by a smoothing spline method. The asymmetry of the magnetization transfer rate (MTR) as determined by $MTR_{asym}(\delta) = MTR(+\delta) - MTR(-\delta)$ was integrated over the offset range from 0.5 - 2ppm, which corresponds to the resonance signal distribution from exchangeable GAG -OH protons, and used as signal intensity for gagCEST images. For quantitative biochemical analysis of absolute GAG content in cartilage, as gold standard, the tibial and talar cartilage compartments were divided into three segments (lateral, central, medial) with 1cm width in the sagittal plane (Fig. 1a). In each segment, 5 contiguous cartilage samples were taken, and a GAG assay (Blyscan B3000 GAG Assay) was used to determine absolute GAG content (μ g/mg) and water content of the probes. The calculated GAG concentrations were expressed as the relative weight per cartilage wet weight [% GAG/mg WWt]. To compare MRI data to biochemical analysis, cartilage areas were segmented in MR images and gagCEST values were averaged in regions corresponding to the division used for biochemical analysis. The correlation coefficient (r) for gagCEST and biochemical assay was determined using Pearson correlation analysis. To account for individual differences in cartilage water content, which can alter chemical exchange effects, measured gagCEST signals were scaled to the fictive case of 90 % water content in cartilage.

Results: All examined ankles showed morphologically intact cartilage on PD_w MR images. From the 42 available cartilage samples (7 patients \times 2 cartilage surfaces \times 3 cartilage segments = 42), 4 samples from ankle # 6 were excluded from analysis due to extremely thin (\ll 0.8 mm) cartilage in the medial and lateral segments. The remaining 38 data points showed a linear correlation between gagCEST signal intensities and GAG concentrations with $r = 0.797$ if differences in water contents were neglected. If these differences were accounted for,

a higher correlation coefficient of $r = 0.859$ was obtained (Fig. 1b). The average measured gagCEST signal intensity (Fig. 1c) was 5.47 ± 3.52 % (mean \pm SD), and 8.11 ± 5.32 % with normalized water content. The average GAG content as determined by biochemical analysis was 6.49 ± 1.14 % GAG/mg WWt. The relative water content in cartilage had a mean of 68.85 ± 4.54 %.

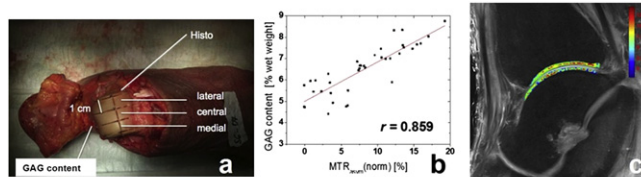


Fig. 1: (a) Axial view on the talus of a cadaver demonstrating the segmentation of cartilage for biochemical assay. (b) Biochemically determined cartilage GAG content plotted against gagCEST signal intensities measured in segmented cartilage revealing a linear correlation of $r = 0.859$. (c) Overlay of sagittal proton-density weighted MR image with gagCEST signal intensities in tibial and talar cartilage showing consistent signal distribution in cartilage areas.

Conclusions: The linear correlation between gagCEST signal intensities and cartilage GAG content is in agreement with CEST theory, which yields that CEST effects scale linearly with the concentration of exchanging protons in bulk water. Thus, our results indicate that gagCEST imaging at 3 T is sensitive to cartilage GAG content in intact tissue samples, and GAG quantification can be improved by taking into account the relative water content in cartilage. Although the initial results from this study suggest a potential of gagCEST imaging for clinical assessment of cartilage GAG content, further studies, involving larger numbers of patients and a larger variance of cartilage GAG content are needed to evaluate the clinical relevance of the technique, also in comparison to other PG sensitive imaging techniques.

439 SEPARATE QUANTITATIVE FEATURES OF EARLY RADIOGRAPHIC KNEE OSTEOARTHRITIS: DEVELOPMENT OVER FIVE YEARS AND RELATION WITH SYMPTOMS IN THE CHECK COHORT

M.B. Kinds¹, A.C. Marijnissen¹, J.W. Bijlsma¹, M. Boers², F.P. Lafeber¹, P.M. Welsing¹. ¹Univ. Med. Ctr. Utrecht, Utrecht, Netherlands; ²VU Univ. Med. Ctr., Amsterdam, Netherlands

Purpose: To evaluate whether quantitative measurement of knee radiographs enables identification of different domains of joint damage in very early osteoarthritis (OA), important for the evaluation of onset and progression of OA. And to evaluate whether these radiographic features progress, are related with each other and with clinical characteristics during five-year follow-up in early OA.

Methods: Knee radiographs from the Cohort Hip & Cohort Knee (CHECK; $n=1002$ participants) were evaluated with Knee Images Digital Analysis (KIDA). CHECK is a prospective study (ten-year) on early OA in ten Dutch hospitals. Separate radiographs of both knees from baseline, two-year and five-year follow-up (T0, T2y, and T5y respectively) were evaluated. KIDA measurement provides per radiograph 14 parameters of joint damage (lateral, medial, and minimum joint space width (JSW), subchondral bone density in lateral and medial femur and tibia, osteophytes on lateral and medial femur and tibia, height of two eminences, varus angle). A principal component analysis aided decisions on how to best combine the KIDA parameters into domains that represent specific separate radiographic OA characteristics. These features were evaluated for development, and were related to each other and to clinical outcome using T0, T2y, and T5y radiographs.

Results: In this cohort with very early symptoms related to OA, minimum JSW, medial JSW, lateral JSW, varus angle (+: varus), osteophyte area (sum of lateral and medial femur, and lateral and medial tibia), eminence height (sum of lateral and medial eminence), and bone density (mean of lateral and medial femur and tibia) were identified as radiographic features. The features progressed in radiographic severity (figure) at different times in follow-up: early (medial JSW, osteophyte area), late (minimum and lateral JSW, eminence height), and both early and late (varus angle, bone density). The separate radiographic features were statistically significantly ($p < 0.05$)

correlated to each other, and correlations varied between different time points. The JSW features were most strongly related to each other (up to $r=0.82$), but also e.g. osteophytes and bone density were significantly correlated (largest $r=0.33$). The relations with clinical outcome varied over time, and relations were most commonly found for osteophyte area and JSW. E.g. the presence of pain at T0 was associated with minimum, medial, and lateral JSW, varus angle, osteophyte area, and eminence height at T0 (odds ratio; OR=0.81, 0.70, 1.38, 0.74, 1.43, and 1.08 respectively). At T2y pain presence was associated with lateral JSW, varus angle, and osteophyte area (OR=0.87, 1.17, 1.42), and at T5y associations were found with minimum JSW, osteophyte area, and bone density (OR=0.79, 1.47, and 1.04). Radiographic features were also associated with WOMAC (Western Ontario & McMaster Universities) pain and function score at different time points.

Conclusions: The separate radiographic features, which were identified by quantitative measurement with KIDA, all progressed over five years in this early OA cohort. Progression occurred at different rates between time points. The relations between the radiographic features and with clinical outcome varied over time. This implies that longitudinal evaluation of separate features will give further insight in OA progression.

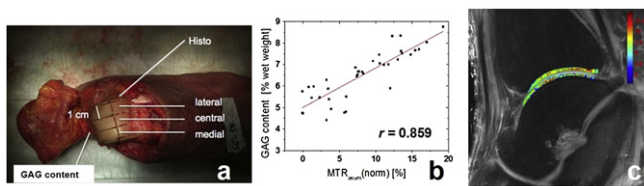


Fig. 1: (a) Axial view on the talus of a cadaver demonstrating the segmentation of cartilage for biochemical assay. (b) Biochemically determined cartilage GAG content plotted against gagCEST signal intensities measured in segmented cartilage revealing a linear correlation of $r = 0.859$. (c) Overlay of sagittal proton-density weighted MR image with gagCEST signal intensities in tibial and talar cartilage showing consistent signal distribution in cartilage areas.

440 MICROSTRUCTURE ANALYSIS OF SUBCHONDRAL TRABECULAR BONE IN HIP OSTEOARTHRITIS - EX-VIVO HR-PQCT STUDY -

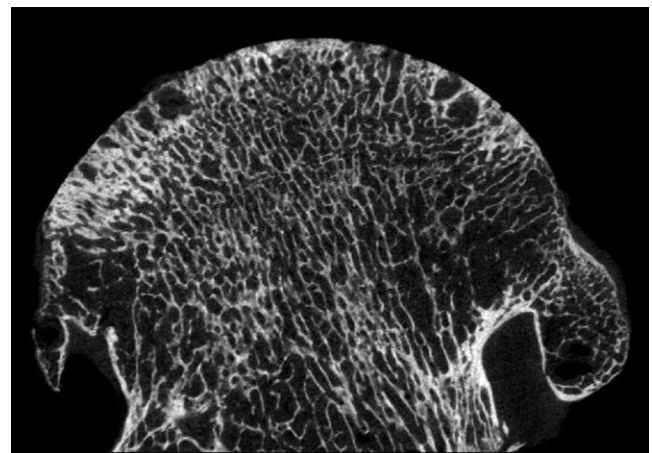
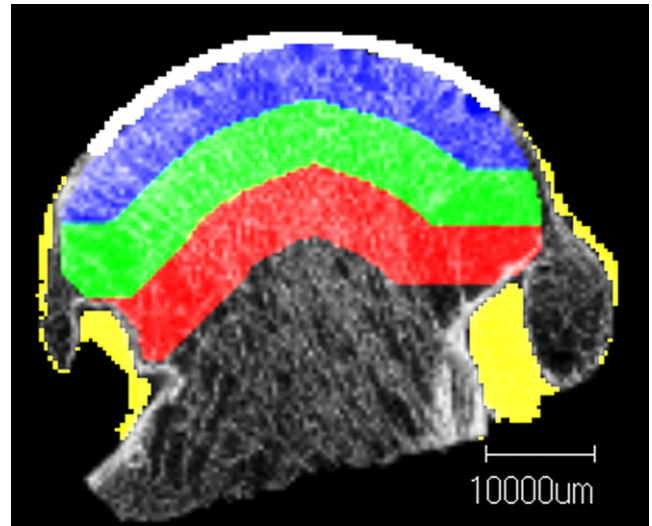
K. Chiba, A. Burghardt, S. Majumdar. *Univ. of California, San Francisco, San Francisco, CA, USA*

Purpose: Abnormalities of bone structure and metabolism in subchondral bone are thought to be deeply involved in pathophysiology of osteoarthritis (OA). To investigate microstructural features of OA subchondral bone, we performed ex-vivo analysis of femoral heads in hip OA patients using High Resolution peripheral Quantitative CT (HR-pQCT).

Methods: Femoral head specimens extracted from 10 hip OA patients (average 73 y.o, all female, terminal stage) were studied. HR-pQCT (Xtreme CT, Scanco medical) scan was performed at $41\mu\text{m}$ voxel size. Subchondral trabecular bone was divided into three layers: 0–5 mm, 5–10 mm, and 10–15 mm under weight-bearing area of femoral head, and the microstructural parameters were measured and compared in each layer. (bone cysts were excluded from the measurement region) (TRI/3D-BON, Ratoc System Engineering, Japan).

Results: Bone volume fraction were average 49.9% in layer 0–5 mm, 24.4% in layer 5–10 mm, and 17.8% in layer 10–15 mm. Trabecular thickness were 566, 338, and $305\mu\text{m}$ respectively. Trabecular number were 0.448, 0.462, and 0.445 /mm respectively. Trabecular separation were 459, 630, and $597\mu\text{m}$ respectively.

Discussion: HR-pQCT can perform in-vivo microstructural analysis for human peripheral bone, and by using it ex-vivo, has the advantage of being able to evaluate whole microstructure of relatively large size bone specimens from peripheral and axial sites. In this study, we could analyze microstructural variations of OA subchondral bone extensively and quantitatively. Our data suggested marked osteosclerosis was found particularly in 0–5 mm layer. And increased bone volume fraction in this layer depended on not increased trabecular number but increased trabecular thickness.



441 THE ARTICULAR CARTILAGE THICKNESS OF THE GLENOID IN THE JAPANESE POPULATION: A HISTOLOGICAL ANALYSIS.

K. Imagawa¹, J. Zuo², T. Hatta¹, Y. Itoigawa³, N. Yamamoto¹, H. Sano¹, E. Itoi¹. ¹Dept. of Orthopaedic Surgery, Tohoku Univ. Sch. of Med., Sendai, Japan; ²Dept. of Orthopaedic Surgery, China-Japan Union Hosp. of Jilin Univ., Changchun, China; ³Dept. of Orthopaedic Surgery, Juntendo Univ. Sch. of Med., Tokyo, Japan

Purpose: The morbidity of osteoarthritis (OA) in the shoulder joint is relatively lower compared to other joints. Nakagawa et al reviewed shoulder plain X-ray of 4035 patients and reported the morbidity of shoulder OA was 0.4%. Furthermore, the prevalence of primary shoulder OA in the Japanese population is rare compared to the European or American population. Cartilage thickness may be one explanation for the difference in the prevalence of shoulder OA. The aim of this study is to investigate the glenoid articular cartilage thickness in the Japanese population using histological analysis.

Methods: Fifty-four glenoid specimens were harvested from 15 male and 15 female cadavers with ethical approval. The average age of the cadavers was 81.5 ± 8.8 . When the glenoid samples were taken from the cadavers, absence or presence of rotator cuff tear (RCT) was noted. RCT was present in 8 shoulders. OA grading was recorded using the Collin's macroscopic OA grading system. Histological slides of glenoid samples were obtained and cartilage was visualized by Alcian blue staining. Images were taken using digital camera, and thickness of the glenoid articular cartilage was measured using NIH ImageJ. Neer postulated in 1983 that cuff tear